

From Data to Global Asymptotic Stability of Unknown Large-Scale Networks with Provable Guarantees

Mahdieh Zaker

School of Computing
Newcastle University

mahdieh.zaker@newcastle.ac.uk

Amy Nejati

School of Computing
Newcastle University

amy.nejati@newcastle.ac.uk

Abolfazl Lavaei

School of Computing
Newcastle University

abolfazl.lavaei@newcastle.ac.uk

Abstract

We offer a *compositional data-driven* scheme for synthesizing controllers that ensure global asymptotic stability (GAS) across large-scale interconnected networks, characterized by *unknown* mathematical models. In light of each network's configuration composed of numerous subsystems with smaller dimensions, our proposed framework gathers data from each subsystem's trajectory, enabling the design of *local controllers* that ensure *input-to-state stability (ISS)* properties over subsystems, signified by ISS Lyapunov functions. To accomplish this, we require only a *single input-state* trajectory from each unknown subsystem up to a specified time horizon, fulfilling certain rank conditions. Subsequently, under *small-gain compositional* reasoning, we leverage ISS Lyapunov functions derived from data to offer a *control Lyapunov function (CLF)* for the interconnected network, ensuring GAS certificate over the network. We demonstrate that while the computational complexity for designing a CLF increases *polynomially* with the network dimension using sum-of-squares (SOS) optimization, our compositional data-driven approach significantly mitigates it to *linear* with respect to the number of subsystems. We showcase the efficacy of our data-driven approach over a set of benchmarks, involving physical networks with diverse interconnection topologies.

Keywords

Data-driven control, global asymptotic stability, large-scale network, provable guarantees

1 Introduction

In recent years, significant focus has been directed towards large-scale interconnected networks, driven by their capacity to model a wide array of real-world applications, including, but not limited to, biological networks, transportation systems, and interconnected power grids. The efficiency of an interconnected network relies on how its subsystems interact and contribute to the overall behavior of the network. When an individual subsystem experiences failure or disturbance, it can propagate disruptions across other subsystems, causing significant upheavals in the network's operation.

Input-to-state stability has been essentially employed to investigate robust behaviors of interconnected networks, influenced by disturbances acting as adversarial inputs [1–3]. In particular, the influence of any subsystem on others within an interconnected network can be effectively captured by ISS Lyapunov functions, while constructing interaction gain functions. These functions are instrumental in delineating the interconnection structure of the network and capturing the effect of neighboring subsystems. According to the *small-gain reasoning*, if the constructed gains satisfy

certain compositional conditions, the overall network would exhibit stability [4–7].

Primary Challenge. To conduct stability analysis over interconnected networks using ISS properties, *precise mathematical models* of subsystems are essential. However, this situation is not typical in numerous real-world applications, where system's dynamics are often unknown. To address this challenge, data-driven approaches have emerged in two distinct categories: *indirect* and *direct* [8]. Indirect data-driven approaches aim to approximate unknown dynamics through identification techniques; nonetheless, obtaining an accurate mathematical model can be computationally demanding, particularly for complex nonlinear systems [9]. Even if a model can be identified through system identification approaches, designing a controller that guarantees the input-to-state stability of the identified model remains challenging. Hence, the complexity arises from two layers: (i) model identification, and (ii) controller synthesis using conventional model-based approaches. In contrast, *direct* data-driven techniques aim to circumvent system identification and directly offer formal analysis on the stability of the system solely based on observed data [8].

Background Research. There have been a few studies based on data-driven frameworks to provide stability certificates for unknown dynamical systems. In this context, [10] and [11] propose a data-driven scheme for the stability analysis of persistently excited linear time-invariant and nonlinear polynomial systems, respectively. In [12], a robust data-driven model-predictive control is introduced for linear time-invariant systems. The study in [13] develops a data-driven approach for robust control synthesis of nonlinear systems considering model uncertainty. Additionally, [14] introduces a data-driven approach for learning controllers capable of rapid adaptation to unknown dynamics. In [15], a methodology is introduced for learning a composition of neural network policies in stochastic environments, providing a formal probabilistic certification ensuring the fulfillment of a specification over the policy's behavior. Data-driven stability analysis for unknown systems is presented for switched systems in [16], continuous-time systems in [17], and discrete-time systems in [18]. The work [19] presents a framework for stabilizing unknown nonlinear systems by jointly learning a neural Lyapunov function and a nonlinear controller, ensuring theoretical stability guarantees through the use of Satisfiability Modulo Theories (SMT) solvers. By applying overapproximation techniques to characterize the set of polynomial dynamics that align with the noisy measured data, [20] constructs an ISS Lyapunov function and a corresponding ISS control law for unknown nonlinear input-affine systems with polynomial dynamics. A data-driven method for synthesizing the *incremental*

ISS controllers and certifying the incremental ISS property for unknown nonlinear polynomial systems has recently been explored in [21].

While studies [10–21] focus on stability analysis and controller synthesis using data, their methods are specifically tailored to *monolithic systems* with low dimensions and cannot be directly applied to large-scale networks due to the *sample complexity* problem. Some limited recent efforts aim to address stability analysis for higher-dimensional systems. In particular, the work [22] explores how deep neural networks can approximate control Lyapunov functions for high-dimensional systems, aiming to circumvent the curse of dimensionality. Utilizing the compositional structure inherent in interconnected nonlinear systems, [23] proposes a compositional method to train and validate neural Lyapunov functions for stability analysis. In [24], a compositional approach is employed to provide neural certificates based on ISS Lyapunov functions and controllers for networked dynamical systems. The work [25] provides a data-driven stability certificate for interconnected networks.

While [22–24] provide compositional techniques to ensure stability in large-scale systems, they each assume *known system dynamics*, in contrast to our work which focuses on unknown dynamics—a more challenging scenario that is often the case in reality. Additionally, the ISS Lyapunov functions constructed by neural networks in [24] are merely candidate functions without a correctness guarantee, necessitating an *additional verification step* using SMT solvers such as Z3 [26], dReal [27] or MathSat [28]. However, SMT solvers may fail to terminate [29] or encounter scalability issues depending on the neural network size or system complexity (see [30, Section 5.2]). In contrast, our method provides ISS Lyapunov functions with a correctness guarantee in a single step. Furthermore, the compositional condition in [24] relies on a stringent symmetry assumption regarding the network structure—a restrictive requirement that our approach does not impose.

In contrast to [25], their approach employs a *scenario-based method* that requires data to be *independent and identically distributed (i.i.d.)*. This limitation allows only one input-output data pair per trajectory [31], necessitating the collection of *multiple independent trajectories* (up to millions in practical scenarios) to achieve the desired confidence level, based on a known closed-form relationship among them. However, our approach requires only a *single input-state trajectory* from each subsystem to derive our results. Additionally, [25] restricts the system class to be *homogeneous*, which does not apply to many practical scenarios. Our results, however, apply to nonlinear systems with polynomial dynamics. Furthermore, although [25] solely provides *verification analysis* over an interconnected network, our work offers controller design—a more challenging and useful task—to enforce the global asymptotic stability property over the network.

Additionally, while we provide the GAS certificate for interconnected networks of nonlinear subsystems by incorporating the influence of subsystems on each other within the network topology via adversarial inputs, [10] considers only linear time-invariant systems using a monolithic approach, which cannot enforce the GAS property for high-dimensional systems (exceeding five states). In contrast, our results apply to systems with up to 2000 states (cf. Table 1). Notably, [10] does not also investigate the ISS property. Furthermore, although it examines robustness to measurement

noise, the analysis assumes bounded noise, whereas our results ensure robustness against *unbounded* adversarial inputs.

Original Contributions. Our work introduces an innovative framework in a *compositional data-driven* manner for synthesizing controllers over an *unknown* interconnected network, while ensuring its global asymptotic stability. Our methodology collects a single trajectory from each unknown subsystem, facilitating the design of a local controller alongside an ISS Lyapunov function for each subsystem based on data. By leveraging the *small-gain compositional* reasoning, we then compose *data-driven* ISS Lyapunov functions and construct a *control Lyapunov function* for the interconnected network, thereby ensuring its GAS certificate. While the computational complexity of CLF design, using SOS optimization, escalates *polynomially* with the network dimension, our compositional data-driven approach offers a *linear complexity* concerning the number of subsystems. We employ several benchmarks to demonstrate the applicability of our data-driven approach over some physical networks with different interconnection topologies.

2 Problem description

2.1 Notation

We employ the following notation throughout the paper. Sets of real, positive and non-negative real numbers are denoted by \mathbb{R} , \mathbb{R}^+ , and \mathbb{R}_0^+ , respectively. We denote sets of non-negative and positive integers by $\mathbb{N} := \{0, 1, 2, \dots\}$ and $\mathbb{N}^+ := \{1, 2, \dots\}$, respectively. Given N vectors $x_i \in \mathbb{R}^{n_i}$, $x = [x_1; \dots; x_N]$ denotes the corresponding column vector of dimension $\sum_i n_i$. Moreover, we use $[x_1 \dots x_N]$ and $[A_1 \dots A_N]$ to represent horizontal concatenation of vectors $x_i \in \mathbb{R}^n$ and matrices $A_i \in \mathbb{R}^{n \times m}$ to form $n \times N$ and $n \times mN$ matrices, respectively. We use $\|\cdot\|$ to signify the Euclidean norm of a vector $x \in \mathbb{R}^n$ and the induced 2-norm of a matrix $A \in \mathbb{R}^{n \times m}$. For any square matrix P , $\lambda_{\min}(P)$ and $\lambda_{\max}(P)$ denote minimum and maximum eigenvalues of P , respectively. We use $P > 0$ to represent that a *symmetric* matrix $P \in \mathbb{R}^{n \times n}$ is positive definite, *i.e.*, all its eigenvalues are positive. A (block) diagonal matrix in $\mathbb{R}^{N \times N}$ with diagonal matrix entries (A_1, \dots, A_N) and scalar entries (a_1, \dots, a_N) is denoted by $\text{blkdiag}(A_1, \dots, A_N)$ and $\text{diag}(a_1, \dots, a_N)$, respectively. The construction of a matrix with elements a_{ij} in the i -th row and j -th column is denoted by $\{a_{ij}\}$. A column vector in \mathbb{R}^n with all elements equal to one is represented by $\mathbb{1}_n$. The transpose of a matrix P is denoted by P^\top , while its *left (right) pseudoinverse* is represented as P^\dagger (P^\ddagger). We denote an $n \times n$ identity matrix by \mathbb{I}_n . A function $\beta : \mathbb{R}_0^+ \rightarrow \mathbb{R}_0^+$ is classified as a \mathcal{K} function if it is continuous, strictly increasing, and satisfies $\beta(0) = 0$, while it belongs to the class \mathcal{K}_∞ if it approaches infinity as its argument tends to infinity. A function $\beta : \mathbb{R}_0^+ \times \mathbb{R}_0^+ \rightarrow \mathbb{R}_0^+$ is considered to be in the class \mathcal{KL} if, for each fixed s , $\beta(r, s)$ is a \mathcal{K} function with respect to r , and for each fixed $r > 0$, $\beta(r, s)$ is decreasing with respect to s , and it approaches 0 as s tends to infinity.

2.2 Individual Subsystems

In this work, we characterize each subsystem as a continuous-time nonlinear polynomial system, as elucidated in the subsequent definition.

Definition 2.1. A continuous-time nonlinear polynomial system (ct-NPS) is described by

$$\Sigma_i: \dot{x}_i = A_i \mathcal{F}_i(x_i) + B_i u_i + D_i w_i, \quad (1)$$

where $\mathcal{F}_i(x_i) \in \mathbb{R}^{N_i}$ is a vector of monomials in states $x_i \in \mathbb{R}^{n_i}$, with $\mathcal{F}_i(0) = 0$, $A_i \in \mathbb{R}^{n_i \times N_i}$ is the system matrix, $B_i \in \mathbb{R}^{n_i \times m_i}$ is the control matrix, and $D_i \in \mathbb{R}^{n_i \times \sigma_i}$ is the adversarial matrix with $\sigma_i = \sum_{j=1, j \neq i}^M n_j$, where M is the number of subsystems. In addition, $u_i \in \mathbb{R}^{m_i}$ denotes the *control* input, and $w_i \in \mathbb{R}^{\sigma_i}$ represents the *adversarial* input of ct-NPS. We employ the tuple $\Sigma_i = (A_i, B_i, D_i, \mathbb{R}^{n_i}, \mathbb{R}^{N_i}, \mathbb{R}^{m_i}, \mathbb{R}^{\sigma_i})$ to denote the subsystem in (1).

In the context of our data-driven work, both matrices A_i and B_i are *unknown*, while matrix D_i is considered known as it captures the weights of interconnections among subsystems, which are often a-priori known in interconnected networks. Moreover, we let $\mathcal{F}_i(x_i)$ include all monomials up to a maximum degree, which can be inferred in ascending order based on physical insights into the unknown system. This approach ensures that $\mathcal{F}_i(x_i)$ potentially includes all monomial terms present in the actual unknown subsystem.

Given that the primary focus of this work is to conduct stability analysis over interconnected networks consisting of individual subsystems in the form of (1), in the following subsection, we present the network structure and elucidate how subsystems can be interconnected.

2.3 Interconnected Network

Here, we provide a formal definition of interconnection between subsystems Σ_i . Let us consider an interconnected network Σ , comprising $M \in \mathbb{N}^+$ subsystems Σ_i , with adversarial inputs and their corresponding matrices partitioned as

$$w_i = [w_{i1}; \dots; w_{i(i-1)}; w_{i(i+1)}; \dots; w_{iM}], \quad (2)$$

$$D_i = [D_{i1} \ \dots \ D_{i(i-1)} \ D_{i(i+1)} \ \dots \ D_{iM}], \quad (3)$$

where $D_{ij} \in \mathbb{R}^{n_i \times n_j}$. We assume the dimension of w_{ij} matches that of x_j , a well-defined assumption in the context of small-gain reasoning. If there is no connection from subsystem Σ_j to Σ_i , it implies that the corresponding adversarial input is identically zero, i.e., $w_{ij} \equiv 0$, otherwise, $w_{ij} = x_j$.

In the interconnected network, *adversarial* inputs and states of subsystems interact mutually, where the states of one subsystem influences an adversarial input of another (cf. interconnection constraint (4)). On the contrary, *control* inputs are those not involved in constructing the interconnection: the GAS property is defined over states, while the primary aim is to design control inputs that ensure such desired property. Now, we proceed with defining an interconnected network.

Definition 2.2. Consider $M \in \mathbb{N}^+$ subsystems $\Sigma_i = (A_i, B_i, D_i, \mathbb{R}^{n_i}, \mathbb{R}^{N_i}, \mathbb{R}^{m_i}, \mathbb{R}^{\sigma_i})$, $i \in \{1, \dots, M\}$, with the adversarial inputs partitioned as in (2). Let us interconnect subsystems Σ_i , $i \in \{1, \dots, M\}$, with the following interconnection constraint:

$$w_{ij} = x_j, \quad \forall i, j \in \{1, \dots, M\}, \quad i \neq j. \quad (4)$$

Then $\Sigma = \mathcal{I}(\Sigma_1, \dots, \Sigma_M)$ is an interconnected network of Σ_i , described by

$$\Sigma: \dot{x} = A\mathcal{F}(x) + Bu, \quad (5)$$

where $A \in \mathbb{R}^{n \times N}$, with $n := \sum_{i=1}^M n_i$, $N := \sum_{i=1}^M N_i$, is an $n \times N$ block matrix with diagonal elements (A_1, \dots, A_M) and off-diagonal elements $\tilde{D}_i = [\tilde{D}_{i1} \ \dots \ \tilde{D}_{i(i-1)} \ \tilde{D}_{i(i+1)} \ \dots \ \tilde{D}_{iM}]$, having values depending on the interconnection topology, where $\tilde{D}_{ij} = [D_{ij} \ \mathbf{0}_{n_i \times (N_j - n_j)}]$, with $\mathbf{0}_{n_i \times (N_j - n_j)}$ being a zero matrix. In addition, $B = \text{blkdiag}(B_1, \dots, B_M) \in \mathbb{R}^{n \times m}$, $u \in \mathbb{R}^m$ with $m := \sum_{i=1}^M m_i$, and $\mathcal{F}(x) = [\mathcal{F}_1(x_1); \dots; \mathcal{F}_M(x_M)] \in \mathbb{R}^N$. We utilize $\Sigma = (A, B, \mathbb{R}^n, \mathbb{R}^N, \mathbb{R}^m)$ to denote the interconnected network in (5).

2.4 GAS Property of Interconnected Network

Here, we first define the global asymptotic stability of an interconnected network [32].

Definition 2.3. An interconnected network $\Sigma = \mathcal{I}(\Sigma_1, \dots, \Sigma_M)$ achieves global asymptotic stability (GAS) if for any $x(0) \in \mathbb{R}^n$ and some function β belonging to the class \mathcal{KL} , the following condition holds:

$$\|x(t)\| \leq \beta(\|x(0)\|, t).$$

This indicates that all solutions of Σ converge to the origin, as its equilibrium point, when time goes to infinity.

We now present the following theorem to demonstrate the required conditions under which an interconnected network achieves GAS according to Definition 2.3.

THEOREM 2.4 ([33]). *Consider an interconnected network $\Sigma = \mathcal{I}(\Sigma_1, \dots, \Sigma_M)$, composed of M subsystems Σ_i . Let there exist a control Lyapunov function (CLF) $\mathcal{V}: \mathbb{R}^n \rightarrow \mathbb{R}_0^+$, and constants $\underline{\alpha}, \bar{\alpha}, \kappa \in \mathbb{R}^+$, such that*

$$\bullet \forall x \in \mathbb{R}^n: \quad \underline{\alpha} \|x\|^2 \leq \mathcal{V}(x) \leq \bar{\alpha} \|x\|^2, \quad (6a)$$

$$\bullet \forall x \in \mathbb{R}^n, \exists u \in \mathbb{R}^m: \quad \mathcal{L}\mathcal{V}(x) \leq -\kappa \mathcal{V}(x), \quad (6b)$$

where $x = [x_1; \dots; x_M]$ and $\mathcal{L}\mathcal{V}$ is the Lie derivative of $\mathcal{V}: \mathbb{R}^n \rightarrow \mathbb{R}_0^+$ with respect to the dynamics in (5), defined as

$$\mathcal{L}\mathcal{V}(x) = \partial_x \mathcal{V}(x)(A\mathcal{F}(x) + Bu), \quad (7)$$

with $\partial_x \mathcal{V}(x) = \frac{\partial \mathcal{V}(x)}{\partial x}$. Then the interconnected network $\Sigma = \mathcal{I}(\Sigma_1, \dots, \Sigma_M)$ is GAS in the sense of Definition 2.3.

In general, searching for a CLF to enforce the GAS property over an interconnected network is often computationally expensive, even if the underlying model is known. To alleviate this, one approach is to analyze the stability of the network by leveraging the *input-to-state* stability property of its underlying subsystems, as defined in the following definition.

Definition 2.5. Given a subsystem Σ_i , the function $\mathcal{V}_i: \mathbb{R}^{n_i} \rightarrow \mathbb{R}_0^+$ is called *input-to-state stable (ISS)* Lyapunov function if there exist constants $\underline{\alpha}_i, \bar{\alpha}_i, \kappa_i \in \mathbb{R}^+, \rho_i \in \mathbb{R}_0^+$, such that

$$\bullet \forall x_i \in \mathbb{R}^{n_i}: \quad \underline{\alpha}_i \|x_i\|^2 \leq \mathcal{V}_i(x_i) \leq \bar{\alpha}_i \|x_i\|^2, \quad (8a)$$

- $\forall x_i \in \mathbb{R}^{n_i}, \exists u_i \in \mathbb{R}^{m_i}$, such that $\forall w_i \in \mathbb{R}^{\sigma_i}$:

$$\mathcal{L}\mathcal{V}_i(x_i) \leq -\kappa_i \mathcal{V}_i(x_i) + \rho_i \|w_i\|^2, \quad (8b)$$

where $\mathcal{L}\mathcal{V}_i$ is the Lie derivative of $\mathcal{V}_i : \mathbb{R}^{n_i} \rightarrow \mathbb{R}_0^+$ with respect to the dynamics in (1), defined as

$$\mathcal{L}\mathcal{V}_i(x_i) = \partial_{x_i} \mathcal{V}_i(x_i) (A_i \mathcal{F}_i(x_i) + B_i u_i + D_i w_i). \quad (9)$$

Using the ISS Lyapunov functions of individual subsystems, a CLF for the interconnected network can be constructed by satisfying a compositional condition (cf. Theorem 4.1), rather than treating the network as a monolithic system. However, constructing these ISS functions is infeasible due to the unknown matrices A_i and B_i appearing in (9). With this primary challenge in place, we can now formally outline the main problem of interest.

PROBLEM 1. Consider an interconnected network $\Sigma = \mathcal{I}(\Sigma_1, \dots, \Sigma_M)$, composed of M subsystems Σ_i , each with unknown matrices A_i and B_i . Construct an ISS Lyapunov function \mathcal{V}_i along with an ISS controller u_i for each unknown subsystem by collecting solely a single input-state trajectory from it. Then, develop a compositional approach based on small-gain reasoning to compose these \mathcal{V}_i and construct a control Lyapunov function \mathcal{V} , along with its associated controller u , across the interconnected network while enforcing its global asymptotic stability.

To address Problem 1, we introduce our data-driven scheme, in the following section, to construct ISS Lyapunov functions for unknown subsystems, derived from data.

3 Data-driven construction of ISS Lyapunov functions

In our data-driven framework, we consider the structure of our ISS Lyapunov function to be quadratic, taking the form $\mathcal{V}_i(x_i) = x_i^\top P_i x_i$, where $P_i > 0$. Subsequently, we gather data from unknown subsystems over the time interval $[t_0, t_0 + (T-1)\tau]$, where $T \in \mathbb{N}^+$ denotes the number of collected samples, and $\tau \in \mathbb{R}^+$ represents the sampling time:

$$\mathcal{U}_i^{0,T} = [u_i(t_0) \ u_i(t_0 + \tau) \ \dots \ u_i(t_0 + (T-1)\tau)], \quad (10a)$$

$$\mathcal{W}_i^{0,T} = [w_i(t_0) \ w_i(t_0 + \tau) \ \dots \ w_i(t_0 + (T-1)\tau)], \quad (10b)$$

$$\mathcal{X}_i^{0,T} = [x_i(t_0) \ x_i(t_0 + \tau) \ \dots \ x_i(t_0 + (T-1)\tau)], \quad (10c)$$

$$\mathcal{X}_i^{1,T} = [\dot{x}_i(t_0) \ \dot{x}_i(t_0 + \tau) \ \dots \ \dot{x}_i(t_0 + (T-1)\tau)]. \quad (10d)$$

We treat trajectories in (10) as a *single input-state trajectory*.

REMARK 1. The state derivatives in $\mathcal{X}_i^{1,T}$ are not directly measurable but are essential for our framework. They can be estimated using numerical approximation based on the derivative definition or through filtering techniques [34, 35]. However, both methods introduce manageable approximation errors, which can be addressed using a strategy similar to [11], as detailed in Subsection 5.2.

Due to the involvement of unknown matrices A_i and B_i in $\mathcal{L}\mathcal{V}_i(x_i)$ in (9), drawing inspiration from [10], we provide the following lemma to derive the data-based representation for $A_i \mathcal{F}_i(x_i) + B_i u_i$.

LEMMA 3.1. Given a subsystem Σ_i , consider a matrix polynomial $G_i(x_i) \in \mathbb{R}^{T \times n_i}$ such that

$$\mathbf{N}_i(x_i) = \mathcal{J}_i^{0,T} G_i(x_i), \quad (11)$$

with $\mathbf{N}_i(x_i) \in \mathbb{R}^{N_i \times n_i}$ being a state-dependent transformation matrix fulfilling

$$\mathcal{F}_i(x_i) = \mathbf{N}_i(x_i) x_i, \quad (12)$$

and $\mathcal{J}_i^{0,T}$ being a full row-rank ($N_i \times T$) matrix, defined as

$$\mathcal{J}_i^{0,T} = [\mathcal{F}_i(x_i(t_0)) \ \mathcal{F}_i(x_i(t_0 + \tau)) \ \dots \ \mathcal{F}_i(x_i(t_0 + (T-1)\tau))]. \quad (13)$$

Then, the data-based counterpart of $A_i \mathcal{F}_i(x_i) + B_i u_i$ is derived as

$$A_i \mathcal{F}_i(x_i) + B_i u_i = (\mathcal{X}_i^{1,T} - D_i \mathcal{W}_i^{0,T}) G_i(x_i) x_i, \\ \text{equivalently:}$$

$$A_i \mathbf{N}_i(x_i) + B_i K_i(x_i) = (\mathcal{X}_i^{1,T} - D_i \mathcal{W}_i^{0,T}) G_i(x_i), \quad (14)$$

by designing the local controllers $u_i = K_i(x_i) x_i = \mathcal{U}_i^{0,T} G_i(x_i) x_i$.

PROOF. From trajectories in (10), we have

$$\mathcal{X}_i^{1,T} = A_i \mathcal{J}_i^{0,T} + B_i \mathcal{U}_i^{0,T} + D_i \mathcal{W}_i^{0,T} = [B_i \ A_i] \begin{bmatrix} \mathcal{U}_i^{0,T} \\ \mathcal{J}_i^{0,T} \end{bmatrix} + D_i \mathcal{W}_i^{0,T}.$$

Accordingly,

$$[B_i \ A_i] \begin{bmatrix} \mathcal{U}_i^{0,T} \\ \mathcal{J}_i^{0,T} \end{bmatrix} = \mathcal{X}_i^{1,T} - D_i \mathcal{W}_i^{0,T}. \quad (15)$$

By utilizing the local controller $u_i = K_i(x_i) x_i = \underbrace{\mathcal{U}_i^{0,T} G_i(x_i) x_i}_{K_i(x_i)}$, one

has

$$A_i \mathcal{F}_i(x_i) + B_i u_i = A_i \mathbf{N}_i(x_i) x_i + B_i u_i = (A_i \mathbf{N}_i(x_i) + B_i K_i(x_i)) x_i \\ = [B_i \ A_i] \begin{bmatrix} K_i(x_i) \\ \mathbf{N}_i(x_i) \end{bmatrix} x_i \\ = [B_i \ A_i] \begin{bmatrix} \mathcal{U}_i^{0,T} \\ \mathcal{J}_i^{0,T} \end{bmatrix} G_i(x_i) x_i. \quad (16)$$

The last equality in (16) is established due to (11) and since $K_i(x_i) = \mathcal{U}_i^{0,T} G_i(x_i)$. Now by applying (15) to (16), we have

$$A_i \mathcal{F}_i(x_i) + B_i u_i = (\mathcal{X}_i^{1,T} - D_i \mathcal{W}_i^{0,T}) G_i(x_i) x_i, \\ \text{equivalently:}$$

$$A_i \mathbf{N}_i(x_i) + B_i K_i(x_i) = (\mathcal{X}_i^{1,T} - D_i \mathcal{W}_i^{0,T}) G_i(x_i),$$

which concludes the proof. \square

REMARK 2. To guarantee that $\mathcal{J}_i^{0,T}$ in (13) achieves full row rank, the number of samples T should not be less than or equal to N_i . This assumption is required to ensure that (11) is feasible and can be readily confirmed since the matrix $\mathcal{J}_i^{0,T}$ is derived from sampled data. This assumption also complies with Willem et al's fundamental lemma [36] regarding the persistently exciting data.

REMARK 3. Note that the full row-rank condition on (13) is necessary and sufficient for the feasibility of (11). To substantiate this claim, we define $G_i(x_i) := \Upsilon_{1i}\Upsilon_{2i}(x_i)$, where $\Upsilon_{1i} \in \mathbb{R}^{T \times N_i}$ and $\Upsilon_{2i}(x_i) \in \mathbb{R}^{N_i \times n_i}$. Since $\mathcal{J}_i^{0,T}$ is assumed to be a full row-rank matrix, its right pseudo-inverse $(\mathcal{J}_i^{0,T})^\ddagger$ always exists. Thus, we can set $\Upsilon_{1i} = (\mathcal{J}_i^{0,T})^\ddagger$ and $\Upsilon_{2i}(x_i) = \mathbf{N}_i(x_i)$. Consequently, this gives $G_i(x_i) = \Upsilon_{1i}\Upsilon_{2i}(x_i) = (\mathcal{J}_i^{0,T})^\ddagger\mathbf{N}_i(x_i)$, leading to $\mathcal{J}_i^{0,T}G_i(x_i) = \mathcal{J}_i^{0,T}(\mathcal{J}_i^{0,T})^\ddagger\mathbf{N}_i(x_i) = \mathbb{I}_{N_i}\mathbf{N}_i(x_i) = \mathbf{N}_i(x_i)$, which confirms the existence of a matrix $G_i(x_i)$ satisfying (11) when $\mathcal{J}_i^{0,T}$ is full row-rank.

By leveraging the data-based representation of $A_i\mathbf{N}_i(x_i) + B_iK_i(x_i)$ as described in Lemma 3.1, we introduce the following theorem, as one of the central contributions of our work, to construct ISS Lyapunov functions alongside their corresponding local controllers directly from data for unknown subsystems.

THEOREM 3.2. Given a ct-NPS Σ_i in (1), with matrices A_i and B_i being unknown, consider the data-based representation (14) as in Lemma 3.1. Let there exist $P_i \in \mathbb{R}^{n_i \times n_i}$ and a matrix polynomial $\Phi_i(x_i) \in \mathbb{R}^{T \times n_i}$ such that

$$\mathcal{J}_i^{0,T}\Phi_i(x_i) = \mathbf{N}_i(x_i)P_i^{-1}, \quad \text{with } P_i > 0. \quad (17a)$$

If

$$C \leq -\kappa_i P_i^{-1}, \quad (17b)$$

where

$$C = (\mathcal{X}_i^{1,T} - D_i\mathcal{W}_i^{0,T})\Phi_i(x_i) + \Phi_i(x_i)^\top(\mathcal{X}_i^{1,T} - D_i\mathcal{W}_i^{0,T})^\top + \pi_i\mathbb{I}_{n_i},$$

for some $\kappa_i, \pi_i \in \mathbb{R}^+$, then $\mathcal{V}_i(x_i) = x_i^\top [\mathbf{N}_i^\dagger \mathcal{J}_i^{0,T} \Phi_i(x_i)]^{-1} x_i$ is an ISS Lyapunov function for Σ_i with $\underline{\alpha}_i = \lambda_{\min}(P_i)$ and $\bar{\alpha}_i = \lambda_{\max}(P_i)$, $\rho_i = \frac{\|D_i\|^2}{\pi_i}$, and $u_i = \mathcal{U}_i^{0,T}\Phi_i(x_i)[\mathbf{N}_i^\dagger \mathcal{J}_i^{0,T} \Phi_i(x_i)]^{-1} x_i$ is its local ISS controller.

PROOF. We first proceed with showing condition (8a). Since

$$\lambda_{\min}(P_i)\|x_i\|^2 \leq \underbrace{x_i^\top [\mathbf{N}_i^\dagger \mathcal{J}_i^{0,T} \Phi_i(x_i)]^{-1} x_i}_{\mathcal{V}_i(x_i)} \leq \lambda_{\max}(P_i)\|x_i\|^2,$$

one can readily satisfy condition (8a) by choosing $\underline{\alpha}_i = \lambda_{\min}(P_i)$ and $\bar{\alpha}_i = \lambda_{\max}(P_i)$.

We now move forward by demonstrating condition (8b), as well. Since $\mathbf{N}_i(x_i)P_i^{-1} = \mathcal{J}_i^{0,T}\Phi_i(x_i)$ according to (17a), then $\mathbf{N}_i(x_i) = \mathcal{J}_i^{0,T}\Phi_i(x_i)P_i$. As $\mathbf{N}_i(x_i) = \mathcal{J}_i^{0,T}G_i(x_i)$ according to (11), then $G_i(x_i) = \Phi_i(x_i)P_i$ can be a proper choice, and accordingly, $G_i(x_i)P_i^{-1} = \Phi_i(x_i)$. Given that $A_i\mathbf{N}_i(x_i) + B_iK_i(x_i) = (\mathcal{X}_i^{1,T} - D_i\mathcal{W}_i^{0,T})G_i(x_i)$ as per Lemma 3.1, we have

$$\begin{aligned} (A_i\mathbf{N}_i(x_i) + B_iK_i(x_i))P_i^{-1} &= (\mathcal{X}_i^{1,T} - D_i\mathcal{W}_i^{0,T}) \underbrace{G_i(x_i)P_i^{-1}}_{\Phi_i(x_i)} \\ &= (\mathcal{X}_i^{1,T} - D_i\mathcal{W}_i^{0,T})\Phi_i(x_i). \end{aligned} \quad (18)$$

By leveraging the definition of Lie derivative in (9), and since $P_i = [\mathbf{N}_i^\dagger \mathcal{J}_i^{0,T} \Phi_i(x_i)]^{-1}$ as per (17a), we have

$$\begin{aligned} \mathcal{L}\mathcal{V}_i(x_i) &= \partial_{x_i}\mathcal{V}_i(x_i)(A_i\mathcal{F}_i(x_i) + B_iu_i + D_iw_i) \\ &= 2x_i^\top P_i(A_i\mathcal{F}_i(x_i) + B_iu_i + D_iw_i) \\ &= 2x_i^\top P_i((A_i\mathbf{N}_i(x_i) + B_iK_i(x_i))x_i + D_iw_i) \\ &= 2x_i^\top P_i(A_i\mathbf{N}_i(x_i) + B_iK_i(x_i))x_i + 2 \underbrace{x_i^\top P_i}_{a_i} \underbrace{D_iw_i}_{b_i}. \end{aligned}$$

Using Cauchy-Schwarz inequality [37] as $a_i^\top b_i \leq \|a_i\|\|b_i\|$, for any $a_i^\top, b_i \in \mathbb{R}^n$, and by leveraging Young's inequality [38] as $\|a_i\|\|b_i\| \leq \frac{\pi_i}{2}\|a_i\|^2 + \frac{1}{2\pi_i}\|b_i\|^2$, for any $\pi_i > 0$, one can attain

$$\begin{aligned} \mathcal{L}\mathcal{V}_i(x_i) &\leq 2x_i^\top P_i(A_i\mathbf{N}_i(x_i) + B_iK_i(x_i))x_i \\ &\quad + \pi_i x_i^\top P_i P_i x_i + \frac{1}{\pi_i} \|D_iw_i\|^2. \end{aligned}$$

By expanding the above expression and factorizing the term $x_i^\top P_i$ from left and $P_i x_i$ from right, and utilizing Cauchy-Schwarz inequality for the last term, we have

$$\begin{aligned} \mathcal{L}\mathcal{V}_i(x_i) &\leq x_i^\top P_i \left[(A_i\mathbf{N}_i(x_i) + B_iK_i(x_i))P_i^{-1} \right. \\ &\quad \left. + P_i^{-1}(A_i\mathbf{N}_i(x_i) + B_iK_i(x_i))^\top + \pi_i \mathbb{I}_{n_i} \right] P_i x_i \\ &\quad + \frac{1}{\pi_i} \|D_i\|^2 \|w_i\|^2. \end{aligned}$$

Since $(A_i\mathbf{N}_i(x_i) + B_iK_i(x_i))P_i^{-1} = (\mathcal{X}_i^{1,T} - D_i\mathcal{W}_i^{0,T})\Phi_i(x_i)$ as per (18), one can conclude that

$$\begin{aligned} \mathcal{L}\mathcal{V}_i(x_i) &\leq x_i^\top P_i \left[(\mathcal{X}_i^{1,T} - D_i\mathcal{W}_i^{0,T})\Phi_i(x_i) \right. \\ &\quad \left. + \Phi_i(x_i)^\top(\mathcal{X}_i^{1,T} - D_i\mathcal{W}_i^{0,T})^\top + \pi_i \mathbb{I}_{n_i} \right] P_i x_i \\ &\quad + \frac{1}{\pi_i} \|D_i\|^2 \|w_i\|^2. \end{aligned}$$

Now, by considering condition (17b), one has

$$\begin{aligned} \mathcal{L}\mathcal{V}_i(x_i) &\leq -\kappa_i x_i^\top P_i \underbrace{P_i^{-1} P_i}_{\mathbb{I}_{n_i}} x_i + \frac{1}{\pi_i} \|D_i\|^2 \|w_i\|^2 \\ &= -\kappa_i \mathcal{V}_i(x_i) + \rho_i \|w_i\|^2, \end{aligned}$$

satisfying condition (8b) with $\rho_i = \frac{\|D_i\|^2}{\pi_i}$. Then one can conclude that $\mathcal{V}_i(x_i) = x_i^\top [\mathbf{N}_i^\dagger \mathcal{J}_i^{0,T} \Phi_i(x_i)]^{-1} x_i$ is an ISS Lyapunov function for Σ_i and $u_i = \mathcal{U}_i^{0,T}\Phi_i(x_i)[\mathbf{N}_i^\dagger \mathcal{J}_i^{0,T} \Phi_i(x_i)]^{-1} x_i$ is its local ISS controller, thereby completing the proof. \square

REMARK 4. Of note is that condition (12) is essential to our approach, as it enables everything to be expressed in terms of x_i rather than $\mathcal{F}_i(x_i)$. This aligns with the structure of our ISS Lyapunov function, $\mathcal{V}_i(x_i) = x_i^\top P_i x_i$, and aids in proving our main results in Theorem 3.2. Given that $\mathcal{F}_i(0) = 0$, there always exists a transformation $\mathbf{N}_i(x_i)$ that meets condition (12), enabling us to define $\mathcal{F}_i(x_i)$ accordingly.

REMARK 5. In order to enforce conditions (17a)-(17b), one can utilize existing software tools in the literature such as SOSTOOLS [39] along with a semidefinite programming (SDP) solver such as SeDuMi [40].

In the next section, we propose a compositional condition using *small-gain reasoning* to construct a control Lyapunov function for the network along with its controller, leveraging ISS Lyapunov functions of its individual subsystems derived from data, thereby ensuring the network's satisfaction of the GAS property.

4 Compositional construction of CLF for interconnected network

We analyze the network $\Sigma = \mathcal{I}(\Sigma_1, \dots, \Sigma_M)$ by deriving a small-gain type compositional condition, exploring the construction of a CLF for the network based on data-driven ISS Lyapunov functions of its subsystems. To do so, we first define $\mathcal{K} := \text{diag}(\kappa_1, \dots, \kappa_M)$ and $\hat{\varrho} := \{\hat{\rho}_{ij}\}$ with $\hat{\rho}_{ij} = \frac{\rho_i}{\alpha_j}$, where $\hat{\rho}_{ii} = 0$, for any $i \in \{1, \dots, M\}$.

We offer the following theorem to demonstrate the conditions under which one can construct a CLF for the unknown network using data-driven ISS Lyapunov functions of the unknown subsystems.

THEOREM 4.1. *Consider a network $\Sigma = \mathcal{I}(\Sigma_1, \dots, \Sigma_M)$, comprised of $M \in \mathbb{N}^+$ subsystems Σ_i . Let each Σ_i possess an ISS Lyapunov function \mathcal{V}_i constructed from data, according to Theorem 3.2. If*

$$\mathbb{1}_M^\top(-\mathcal{K} + \hat{\varrho}) := [\mu_1; \dots; \mu_M]^\top < 0 \quad (19)$$

equivalently, $\mu_i < 0, \forall i \in \{1, \dots, M\}$,

then

$$\mathcal{V}(x) := \sum_{i=1}^M \mathcal{V}_i(x_i) = \sum_{i=1}^M x_i^\top [\mathbf{N}_i^\dagger \mathcal{J}_i^{0,T} \Phi_i(x_i)]^{-1} x_i$$

is a control Lyapunov function for network Σ with

$$\kappa := -\mu, \max_{1 \leq i \leq M} \mu_i < \mu < 0, \quad \underline{\alpha} := \min_i \{\underline{\alpha}_i\}, \quad \bar{\alpha} := \max_i \{\bar{\alpha}_i\}.$$

Moreover, $u = [u_1; \dots; u_M]$ with

$$u_i = \mathcal{U}_i^{0,T} \Phi_i(x_i) [\mathbf{N}_i^\dagger \mathcal{J}_i^{0,T} \Phi_i(x_i)]^{-1} x_i, \quad i \in \{1, \dots, M\},$$

is a controller that renders the network GAS.

PROOF. We first show that condition (6a) is satisfied. According to condition (8a), one has

$$\|x\|^2 = \sum_{i=1}^M \|x_i\|^2 \leq \sum_{i=1}^M \frac{1}{\underline{\alpha}_i} \mathcal{V}_i(x_i) \leq \eta \sum_{i=1}^M \mathcal{V}_i(x_i) = \eta \mathcal{V}(x),$$

where $\eta = \max_i \{\frac{1}{\underline{\alpha}_i}\}$. Then by choosing $\underline{\alpha} = \frac{1}{\eta} = \min_i \{\underline{\alpha}_i\}$, we have

$$\underline{\alpha} \|x\|^2 \leq \mathcal{V}(x).$$

On the other side, we have

$$\mathcal{V}(x) = \sum_{i=1}^M \mathcal{V}_i(x_i) \leq \sum_{i=1}^M \bar{\alpha}_i \|x_i\|^2 \leq \bar{\alpha} \sum_{i=1}^M \|x_i\|^2 = \bar{\alpha} \|x\|^2,$$

with $\bar{\alpha} = \max_i \{\bar{\alpha}_i\}$, implying that condition (6a) is fulfilled with $\underline{\alpha} = \min_i \{\underline{\alpha}_i\}$ and $\bar{\alpha} = \max_i \{\bar{\alpha}_i\}$.

We now proceed with demonstrating that condition (6b) is met, as well. By employing condition (8b), compositional condition $\mathbb{1}_M^\top(-\mathcal{K} + \hat{\varrho}) < 0$, and by defining

$$-\kappa s := \max \{ \mathbb{1}_M^\top(-\mathcal{K} + \hat{\varrho}) \bar{\mathcal{V}}(x) \mid \mathbb{1}_M^\top \bar{\mathcal{V}}(x) = s \},$$

where $\bar{\mathcal{V}}(x) = [\mathcal{V}_1(x_1); \dots; \mathcal{V}_M(x_M)]$, one can obtain the following chain of inequalities:

$$\begin{aligned} \mathbb{L}\mathcal{V}(x) &= \mathbb{L} \sum_{i=1}^M \mathcal{V}_i(x_i) = \sum_{i=1}^M \mathbb{L}\mathcal{V}_i(x_i) \leq \sum_{i=1}^M (-\kappa_i \mathcal{V}_i(x_i) + \rho_i \|w_i\|^2) \\ &= \sum_{i=1}^M (-\kappa_i \mathcal{V}_i(x_i) + \sum_{j=1, j \neq i}^M \rho_{ij} \|w_{ij}\|^2) = \sum_{i=1}^M (-\kappa_i \mathcal{V}_i(x_i) + \sum_{j=1, j \neq i}^M \rho_{ij} \|x_j\|^2) \\ &\leq \sum_{i=1}^M (-\kappa_i \mathcal{V}_i(x_i) + \sum_{j=1, j \neq i}^M \frac{\rho_i}{\alpha_j} \mathcal{V}_j(x_j)) = \sum_{i=1}^M (-\kappa_i \mathcal{V}_i(x_i) + \sum_{j=1, j \neq i}^M \hat{\rho}_{ij} \mathcal{V}_j(x_j)) \\ &= \mathbb{1}_M^\top(-\mathcal{K} + \hat{\varrho}) \underbrace{[\mathcal{V}_1(x_1); \dots; \mathcal{V}_M(x_M)]}_{\bar{\mathcal{V}}(x)} \leq -\kappa \bar{\mathcal{V}}(x). \end{aligned}$$

We now show that $\kappa > 0$ by considering $\kappa = -\mu$. Since $\mathbb{1}_M^\top(-\mathcal{K} + \hat{\varrho}) := [\mu_1; \dots; \mu_M]^\top < 0$, and $\max_{1 \leq i \leq M} \mu_i < \mu < 0$, one has

$$\begin{aligned} -\kappa s &= \mathbb{1}_M^\top(-\mathcal{K} + \hat{\varrho}) \bar{\mathcal{V}}(x) = [\mu_1; \dots; \mu_M]^\top [\mathcal{V}_1(x_1); \dots; \mathcal{V}_M(x_M)] \\ &= \mu_1 \mathcal{V}_1(x_1) + \dots + \mu_M \mathcal{V}_M(x_M) \leq \mu (\mathcal{V}_1(x_1) + \dots + \mathcal{V}_M(x_M)) \\ &= \mu s. \end{aligned}$$

Then, $-\kappa s \leq \mu s$, and accordingly, $-\kappa \leq \mu$ as s is positive. Since $\max_{1 \leq i \leq M} \mu_i < \mu < 0$, then $\kappa = -\mu > 0$, implying that condition (6b) is fulfilled, which completes the proof. \square

We provide Algorithm 1 as a summary of our *compositional data-driven* approach for constructing a CLF and its GAS controller for an unknown network, relying on ISS Lyapunov functions of its individual subsystems.

5 Discussions

5.1 Computational Complexity Analysis

One can leverage SOS optimization programs to impose conditions (17a)-(17b), as illustrated in Remark 5. The computational complexity of SOS is contingent upon both the polynomial degree of candidate Lyapunov functions and the dimension of state variables. Existing research demonstrates that with a fixed degree of Lyapunov functions, computational demands for designing a CLF escalates *polynomially* as the network dimension expands (see, for instance, [29] for a similar argument for barrier functions). In contrast, our compositional data-driven approach substantially mitigates this complexity, scaling *linearly* with the number of subsystems. It is worth mentioning that in our work, the complexity still scales polynomially within each *subsystem level*, but linearly with the number of subsystems, thus making our approach practical for analyzing networks with a large number of subsystems. In particular, the polynomial complexity at the subsystem level is not restrictive in our setting, as we applied our findings to networks with 2000 dimensions, each comprising subsystems of 3 dimensions (cf. Table 1). This expands the applicability of formal data-driven techniques to large-scale networks.

Algorithm 1 Data-driven construction of CLF and its GAS controller

Require: A choice for $\mathcal{F}_i(x_i)$

- 1: **for** $i \in \{1, \dots, M\}$ over the time interval $[t_0, t_0 + (T-1)\tau]$, **do**
- 2: Collect data $\mathcal{U}_i^{0,T}, \mathcal{W}_i^{0,T}, \mathcal{X}_i^{0,T}$, and $\mathcal{X}_i^{1,T}$ using (10a)-(10d)
- 3: Compute $\mathcal{J}_i^{0,T}$ as in (13)
- 4: **end for**
- 5: **for** $i \in \{1, \dots, M\}$, **do**
- 6: Utilize SOSTOOLS and design $\Phi_i(x_i)$ through fulfillment of conditions $\mathcal{J}_i^{0,T} \Phi_i(x_i) = \mathbf{N}_i(x_i) \Xi^1$ in (17a), and $C \leq -\kappa_i \Xi$ in (17b), with $\Xi > 0$, for fixed $\kappa_i, \pi_i \in \mathbb{R}^+$
- 7: Construct ISS Lyapunov function $\mathcal{V}_i(x_i) = x_i^\top [\mathbf{N}_i^\dagger \mathcal{J}_i^{0,T} \Phi_i(x_i)]^{-1} x_i = x_i^\top \Xi^{-1} x_i$ and controller $u_i = \mathcal{U}_i^{0,T} \Phi_i(x_i) [\mathbf{N}_i^\dagger \mathcal{J}_i^{0,T} \Phi_i(x_i)]^{-1} x_i = \mathcal{U}_i^{0,T} \Phi_i(x_i) \Xi^{-1} x_i$
- 8: **end for**
- 9: **if** compositional condition (19) holds **then**
- 10: $\mathcal{V}(x) := \sum_{i=1}^M \mathcal{V}_i(x_i)$ is a CLF for the network Σ , and controller $u = [u_1; \dots; u_M]$ makes the network GAS
- 11: **else**
- 12: Return to Step 1 and repeat the required procedures with a larger dataset comprising more collected samples T
- 13: **end if**

Ensure: CLF $\mathcal{V}(x) = \sum_{i=1}^M x_i^\top [\mathbf{N}_i^\dagger \mathcal{J}_i^{0,T} \Phi_i(x_i)]^{-1} x_i$, controller $u = [u_1; \dots; u_M]$ with $u_i = \mathcal{U}_i^{0,T} \Phi_i(x_i) [\mathbf{N}_i^\dagger \mathcal{J}_i^{0,T} \Phi_i(x_i)]^{-1} x_i$, satisfaction of GAS property across the network

5.2 Limitations

While our proposed approach offers numerous benefits, it also has certain limitations, as is the case with any method, that are worth noting. First, as previously mentioned, we allow $\mathcal{F}_i(x_i)$ to include all monomials up to a maximum degree informed by physical insights into the unknown system. This means $\mathcal{F}_i(x_i)$ may contain extra terms that do not exist in the actual dynamics, potentially making the approach conservative. While the inclusion of these redundant terms can increase computational costs, it ensures that $\mathcal{F}_i(x_i)$ potentially includes all monomial terms present in the actual unknown subsystem, enabling one to provide formal GAS certificates for networks with unknown subsystems. Moreover, this work focuses on polynomial nonlinearities, whereas practical system dynamics may involve broader nonlinear terms, such as fractional, exponential, or trigonometric functions. Extending our results to a wider class of nonlinear systems beyond polynomials is an ongoing research direction.

Another point of note, as briefly mentioned in Remark 1, is that the derivative of states encoded in $\mathcal{X}_i^{1,T}$ cannot be measured directly, whereas their data is required in our framework. Two immediate solutions to overcome this burden are either to obtain their values numerically using $\frac{x_i(t_0+\tau)-x_i(t_0)}{\tau}$ or to employ suitable filters to estimate them via existing approaches [34, 35]. Nevertheless, both

¹By defining $\Xi = P^{-1}$, we address conditions (17a) and (17b) simultaneously so that the product of matrices $\mathcal{J}_i^{0,T}$ and $\Phi_i(x_i)$ yields the product of $\mathbf{N}_i(x_i)$ and a symmetric, positive-definite matrix Ξ , and $C \leq -\kappa_i \Xi$. Subsequently, Ξ equates to the inverse of matrix P , and upon inversion, we obtain matrix P itself.

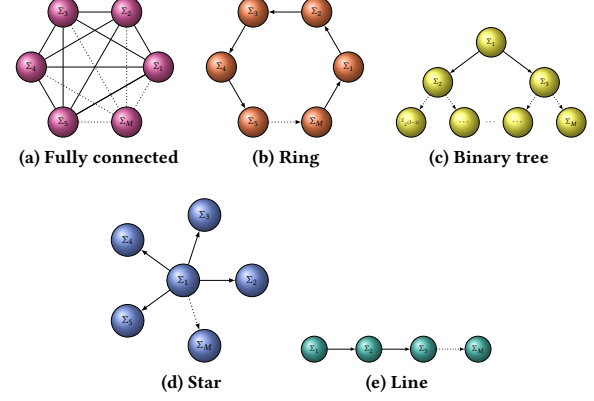


Figure 1: Different interconnection topologies employed in Table 1. In the binary tree topology shown in (c), $M = 2^l - 1$, where l is the number of tree's levels.

methods can introduce approximation errors, which are manageable and not a significant concern. Particularly, a technique similar to that in [11] can be employed to integrate the impact of error in the derivative approximation. More precisely, in this approach, the data $\mathcal{X}_i^{1,T}$ is expressed as $\mathcal{X}_i^{1,T} = \tilde{\mathcal{X}}_i^{1,T} + \Delta_i$, where $\tilde{\mathcal{X}}_i^{1,T}$ represents the error-free data and Δ_i is a small noise capturing the error. The only assumption required is that Δ_i satisfies $\Delta_i \Delta_i^\top \leq \Lambda_i \Lambda_i^\top$ for some known matrix Λ_i , which is a common assumption in control and intuitively indicates that the noise energy during data collection is bounded. We opted not to use this method in the paper for the sake of a clearer presentation and since it does not represent a core contribution of this work.

6 Simulation results

In this section, we demonstrate the effectiveness of our compositional data-driven approach by applying it to three networks: two real-world systems, including spacecraft [41] and chaotic Lorenz-type systems (referred to as Lu) [42], and an academic example, all interconnected via various topologies, as shown in Figure 1. A general yet brief overview of these case studies is provided in Table 1. In all case studies, we assume that the matrices A_i, B_i of subsystems and, accordingly, A and B of the networks are unknown. All simulations are performed in MATLAB R2023b on a MacBook Pro (Apple M2 Pro with 16GB memory).

The primary goal across all case studies is to design a CLF and its GAS controller for the interconnected network with an unknown mathematical model. To accomplish this, under Algorithm 1, we gather input-state trajectories from subsystems as described in (10) and satisfy condition (17b) by constructing ISS Lyapunov functions and local controllers for all subsystems. Then, utilizing the compositionality results from Theorem 4.1, we compositionally design a CLF and its controller for the interconnected network based on ISS Lyapunov functions of subsystems, ensuring the network is GAS. In the subsequent subsections, each case study is presented and the corresponding results are reported.

Table 1: An overview of our data-driven findings across a set of interconnected networks, including runtime (RT) and memory usage (MU), required for each subsystem. M represents the number of subsystems, and T denotes the number of collected samples.

System	Selected $\mathcal{F}_i(x_i)$	Network parameters			Computation costs	
		Topology	M	T	RT (sec)	MU (Mb)
Spacecraft	$[x_{1i}; x_{2i}; x_{3i}; x_{1i}^2; x_{2i}^2; x_{3i}^2; x_{1i}x_{2i}; x_{1i}x_{3i}; x_{2i}x_{3i}]$	Fully connected	1000	100	< 1	3.54
		Ring	2000	15	< 1	< 1
Academic network	$[x_{1i}; x_{2i}; x_{1i}^2; x_{2i}^2; x_{1i}x_{2i}]$	Binary tree	2047	12	< 1	< 1
		Star	1000	10	< 1	< 1
Lu	$[x_{1i}; x_{2i}; x_{3i}; x_{1i}x_{3i}; x_{1i}x_{2i}; x_{2i}x_{3i}]$	Line	2000	150	< 1	1.41

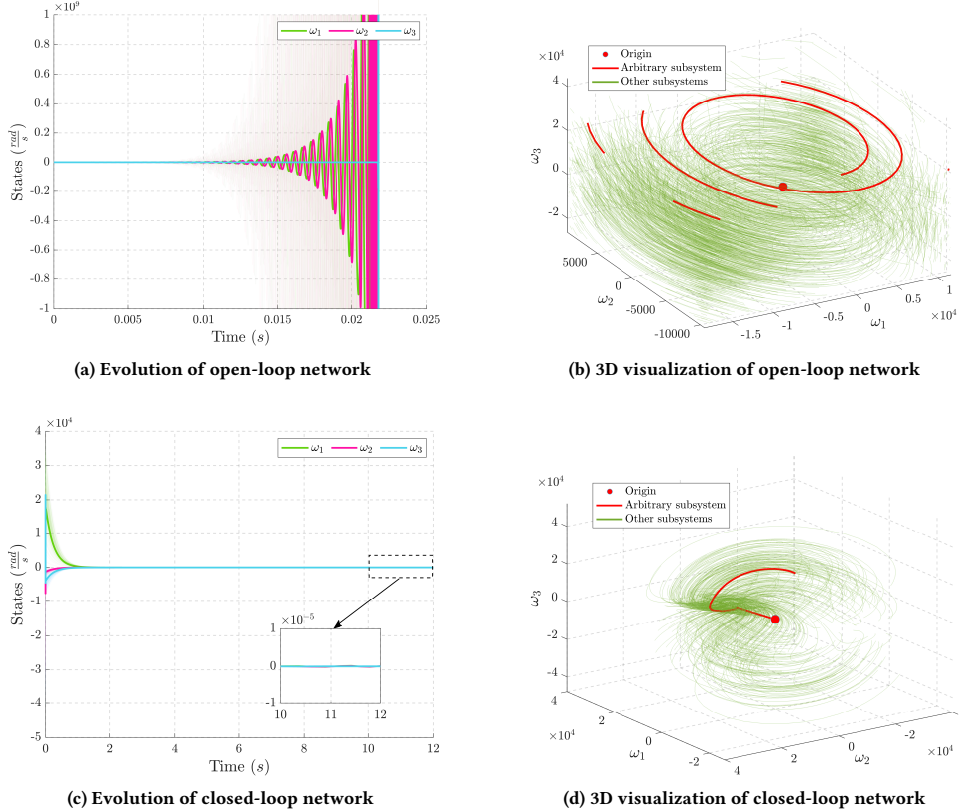


Figure 2: Interconnected spacecraft network in a fully-interconnected topology: (a) and (b) depict the network's behavior without the controller, resulting in diverging trajectories. (c) illustrates the network's evolution under the synthesized controller, highlighting the states of an arbitrary subsystem in bold and shading those of the remaining subsystems. (d) visualizes trajectories of the network under the synthesized controller in 3D, demonstrating that all states converge to the origin.

6.1 Spacecraft Network: Fully-interconnected Topology

The first case study is a fully-interconnected network of 1000 rotating rigid spacecraft² [41]. Each spacecraft has three states $x_i = [x_{1i}; x_{2i}; x_{3i}]$, which are the angular velocities ω_{1i} to ω_{3i} along the principal axes and are affected by those of its neighboring

²While we assume all subsystems are identical for simplicity, our proposed results are applicable to networks with heterogeneous subsystems.

subsystems. Each subsystem is described by the following dynamics

$$\begin{aligned} \dot{x}_{1i} &= \frac{(J_{2i} - J_{3i})}{J_{1i}} x_{2i} x_{3i} + \frac{1}{J_{1i}} u_{1i} - 10^{-4} \sum_{\substack{j=1 \\ j \neq i}}^{1000} x_{3j}, \\ \dot{x}_{2i} &= \frac{(J_{3i} - J_{1i})}{J_{2i}} x_{1i} x_{3i} + \frac{1}{J_{2i}} u_{2i} - 10^{-4} \sum_{\substack{j=1 \\ j \neq i}}^{1000} x_{1j}, \\ \dot{x}_{3i} &= \frac{(J_{1i} - J_{2i})}{J_{3i}} x_{1i} x_{2i} + \frac{1}{J_{3i}} u_{3i} - 10^{-4} \sum_{\substack{j=1 \\ j \neq i}}^{1000} x_{2j}, \end{aligned} \quad (20)$$

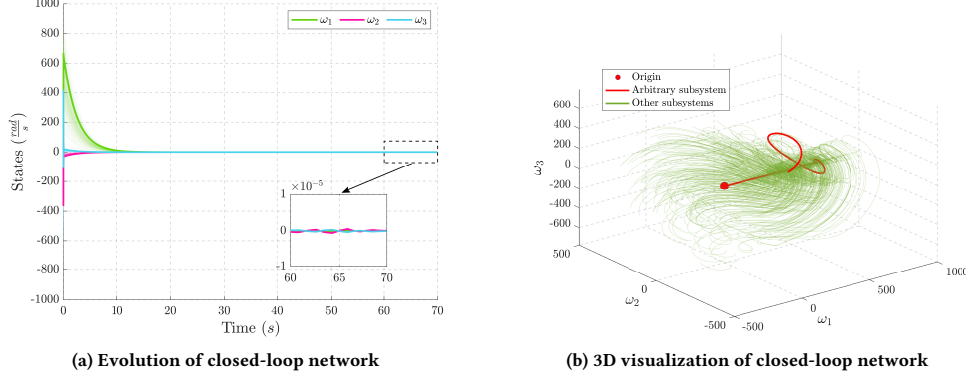


Figure 3: Interconnected spacecraft network in a ring topology: (a) demonstrates the evolution of the network under the synthesized controller, highlighting the states of an arbitrary subsystem in bold and shading those of the remaining subsystems. (b) visualizes trajectories of the network under the synthesized controller in 3D, demonstrating that all states converge to the origin.

where $u_i = [u_{1i}; u_{2i}; u_{3i}]$ is the torque input, and J_{1i} to J_{3i} are the principal moments of inertia. Considering $\mathcal{F}_i(x_i) = [x_{1i}; x_{2i}; x_{3i}; x_{2i}x_{3i}; x_{1i}x_{3i}; x_{1i}x_{2i}]$ as the actual monomials of each subsystem, unknown matrices

$$A_i = \begin{bmatrix} 0 & 0 & 0 & \frac{(J_{2i}-J_{3i})}{J_{1i}} & 0 & 0 \\ 0 & 0 & 0 & 0 & \frac{(J_{3i}-J_{1i})}{J_{2i}} & 0 \\ 0 & 0 & 0 & 0 & 0 & \frac{(J_{1i}-J_{2i})}{J_{3i}} \end{bmatrix},$$

$$B_i = \begin{bmatrix} \frac{1}{J_{1i}} & 0 & 0 \\ 0 & \frac{1}{J_{2i}} & 0 \\ 0 & 0 & \frac{1}{J_{3i}} \end{bmatrix},$$

and the adversarial matrix partitions

$$D_{ij} = 10^{-4} \times \begin{bmatrix} 0 & 0 & -1 \\ -1 & 0 & 0 \\ 0 & -1 & 0 \end{bmatrix},$$

according to Definition 2.2 for a fully-interconnected topology, we have

$$A = \begin{bmatrix} A_1 & \tilde{D}_{12} & \tilde{D}_{13} & \cdots & \tilde{D}_{1\ 1000} \\ \tilde{D}_{21} & A_2 & \tilde{D}_{23} & \cdots & \tilde{D}_{2\ 1000} \\ \vdots & & \ddots & & \vdots \\ \tilde{D}_{999\ 1} & \cdots & \tilde{D}_{999\ 998} & A_{999} & \tilde{D}_{999\ 1000} \\ \tilde{D}_{1000\ 1} & \cdots & \tilde{D}_{1000\ 998} & \tilde{D}_{1000\ 999} & A_{1000} \end{bmatrix},$$

$$B = \text{blkdiag}(B_1, \dots, B_{1000}).$$

Figures 2(a) and 2(b) depict the network's behavior in the absence of a controller (open-loop). To avoid such behavior, we construct a CLF and its associated controller utilizing our data-driven framework. To do so, we gather $T = 100$ samples with $\tau = 0.01$ from each subsystem (20) and choose $\mathcal{F}_i(x_i) = [x_{1i}; x_{2i}; x_{3i}; x_{1i}^2; x_{2i}^2; x_{3i}^2; x_{1i}x_{2i}; x_{1i}x_{3i}; x_{2i}x_{3i}]$. Following the steps in Algorithm 1, we set $\kappa_i = 0.1$, $\pi_i = 0.71578$ and design

$$P_i = \begin{bmatrix} 4.8315 & 0.9437 & -0.0149 \\ 0.9437 & 3.4773 & -0.2598 \\ -0.0149 & -0.2598 & 2.8181 \end{bmatrix},$$

$$\begin{aligned} \mathcal{V}_i(x_i) &= 4.8315x_{1i}^2 + 1.8873x_{1i}x_{2i} - 0.029784x_{1i}x_{3i} + 3.4773x_{2i}^2 \\ &\quad - 0.51959x_{2i}x_{3i} + 2.8181x_{3i}^2, \\ u_{1i} &= -7.2915x_{1i}^2 + 0.095205x_{1i}x_{2i} - 30.3111x_{1i}x_{3i} + 99.6962x_{2i}^2 \\ &\quad - 33.8855x_{2i}x_{3i} + 46.4852x_{3i}^2 - 812.734x_{1i} - 124.5246x_{2i} \\ &\quad + 6.5823x_{3i}, \\ u_{2i} &= 37.0636x_{1i}^2 - 135.3413x_{1i}x_{2i} + 115.2349x_{1i}x_{3i} - 27.1295x_{2i}^2 \\ &\quad + 34.5258x_{2i}x_{3i} + 0.39821x_{3i}^2 - 206.8314x_{1i} - 605.312x_{2i} \\ &\quad + 46.1622x_{3i}, \\ u_{3i} &= -25.567x_{1i}^2 - 83.3144x_{1i}x_{2i} - 90.2213x_{1i}x_{3i} - 1.4901x_{2i}^2 \\ &\quad - 20.3337x_{2i}x_{3i} + 0.42353x_{3i}^2 - 29.969x_{1i} + 57.9927x_{2i} \\ &\quad - 710.6459x_{3i}, \end{aligned}$$

with $\underline{\alpha}_i = 2.6603$, $\bar{\alpha}_i = 5.3229$, $\rho_i = 1.3957 \times 10^{-5}$, which satisfies the compositional condition (19). Hence, the CLF and GAS controller for the network are obtained as

$$\mathcal{V}(x) = \sum_{i=1}^{1000} \mathcal{V}_i(x_i), \quad u = [u_1; \dots; u_{1000}],$$

with $\underline{\alpha} = \min_i \{\underline{\alpha}_i\} = 2.6603$, $\bar{\alpha} = \max_i \{\bar{\alpha}_i\} = 5.3229$, and $\kappa = 0.0948$.

We apply the GAS controller to the network with arbitrary initial conditions $x(0) \in [-25000, 25000]$, which are large enough to evidence the efficacy of our proposed approach. Figures 2(c) and 2(d) show the closed-loop trajectories of a representative spacecraft subsystem in a fully-interconnected topology under the synthesized controller.

REMARK 6. In our case studies, we assumed error-free state derivative data. However, if state derivatives are approximated, the imposed

error $(\Delta_i \Delta_i^\top)$ is bounded by $(\Lambda_i \Lambda_i^\top)$ (as discussed in Subsection 5.2). In this case, (17b) should be adjusted to incorporate the error, ensuring robustness at the cost of increased conservatism in satisfying the condition.

6.2 Spacecraft Network: Ring Topology

Here, we consider a ring network of 2000 spacecrafts. Each subsystem is described by

$$\begin{aligned}\dot{x}_{1i} &= \frac{(J_{2i} - J_{3i})}{J_{1i}} x_{2i} x_{3i} + \frac{1}{J_{1i}} u_{1i} - 10^{-4} x_{3(i-1)}, \\ \dot{x}_{2i} &= \frac{(J_{3i} - J_{1i})}{J_{2i}} x_{1i} x_{3i} + \frac{1}{J_{2i}} u_{2i} - 10^{-4} x_{1(i-1)}, \\ \dot{x}_{3i} &= \frac{(J_{1i} - J_{2i})}{J_{3i}} x_{1i} x_{2i} + \frac{1}{J_{3i}} u_{3i} - 10^{-4} x_{2(i-1)},\end{aligned}\quad (21)$$

for $i \in \{2, \dots, 2000\}$, where the first subsystem is affected by the last subsystem. The matrices of the ring network as per Definition 2.2 are as follows:

$$A = \begin{bmatrix} A_1 & \mathbf{0}_{3 \times 6} & \mathbf{0}_{3 \times 6} & \cdots & \tilde{D}_{1 \ 2000} \\ \tilde{D}_{21} & A_2 & \mathbf{0}_{3 \times 6} & \cdots & \mathbf{0}_{3 \times 6} \\ \vdots & & \ddots & & \vdots \\ \mathbf{0}_{3 \times 6} & \cdots & \tilde{D}_{1999 \ 1998} & A_{1999} & \mathbf{0}_{3 \times 6} \\ \mathbf{0}_{3 \times 6} & \cdots & \mathbf{0}_{3 \times 6} & \tilde{D}_{2000 \ 1999} & A_{2000} \end{bmatrix},$$

$B = \text{blkdiag}(B_1, \dots, B_{2000})$.

We collect $T = 15$ samples with a sampling time of $\tau = 0.01$ from each subsystem in (21). Following the procedure outlined in Algorithm 1, we set $\kappa_i = 10^{-6}$ and $\pi_i = 0.00077986$, obtaining the following results:

$$P_i = \begin{bmatrix} 318.1693 & -19.1415 & 49.8083 \\ -19.1415 & 857.7995 & 184.3652 \\ 49.8083 & 184.3652 & 505.8565 \end{bmatrix},$$

$$\begin{aligned}\mathcal{V}_i(x_i) &= 318.1693 x_{1i}^2 - 38.2831 x_{1i} x_{2i} + 99.6167 x_{1i} x_{3i} \\ &\quad + 857.7995 x_{2i}^2 + 368.7303 x_{2i} x_{3i} + 505.8565 x_{3i}^2, \\ u_{1i} &= 0.11777 x_{1i}^2 + 16.3415 x_{1i} x_{2i} + 12.7878 x_{1i} x_{3i} + 80.6853 x_{2i}^2 \\ &\quad + 63.0886 x_{2i} x_{3i} + 15.6556 x_{3i}^2 - 77.3744 x_{1i} + 5.4254 x_{2i} \\ &\quad + 9.8153 x_{3i}, \\ u_{2i} &= -2.6059 x_{1i}^2 - 16.1453 x_{1i} x_{2i} - 40.3623 x_{1i} x_{3i} + 4.0518 x_{2i}^2 \\ &\quad + 4.9017 x_{2i} x_{3i} + 17.1156 x_{3i}^2 + 12.9201 x_{1i} - 206.6947 x_{2i} \\ &\quad + 19.7909 x_{3i}, \\ u_{3i} &= -2.6307 x_{1i}^2 - 88.7645 x_{1i} x_{2i} - 47.1421 x_{1i} x_{3i} - 15.7124 x_{2i}^2 \\ &\quad - 35.6218 x_{2i} x_{3i} - 11.6692 x_{3i}^2 - 3.8432 x_{1i} + 107.8112 x_{2i} \\ &\quad - 141.9266 x_{3i},\end{aligned}$$

with $\underline{\alpha}_i = 296.3880$, $\bar{\alpha}_i = 936.7001$, $\rho_i = 1.2823 \times 10^{-5}$. These parameters satisfy the compositional condition (19), yielding $\underline{\alpha} = \min_i \{\underline{\alpha}_i\} = 296.3880$, $\bar{\alpha} = \max_i \{\bar{\alpha}_i\} = 936.7001$, and $\kappa = 9.5674 \times 10^{-7}$. Consequently, the CLF and GAS controller for the network

are given by

$$\mathcal{V}(x) = \sum_{i=1}^{2000} \mathcal{V}_i(x_i), \quad u = [u_1; \dots; u_{2000}].$$

We apply the GAS controller to the network with arbitrary initial conditions $x(0) \in [-400, 400]$. Figures 3(a) and 3(b) show the closed-loop trajectories of a representative spacecraft subsystem in a ring topology under the synthesized controller, verifying the efficacy of our approach.

6.3 Academic Network: Binary Tree Topology

Another case study involves a binary tree network of 2047 subsystems of an academic example. Each subsystem has two states $x_i = [x_{1i}; x_{2i}]$, and is described by the following dynamics:

$$\begin{aligned}\dot{x}_{1i} &= x_{2i} + 10^{-2} \Pi(i = 2j \vee i = 2j + 1) x_{1j}, \\ \dot{x}_{2i} &= x_{1i}^2 + u_i,\end{aligned}\quad (22)$$

where u_i is the control input, and Π is an indicator function defined as

$$\Pi(i = 2j \vee i = 2j + 1) = \begin{cases} 1 & i = 2j \vee i = 2j + 1, \\ 0 & \text{Otherwise.} \end{cases}$$

with \vee being the logical OR operation. Then, considering $\mathcal{F}_i(x_i) = [x_{1i}; x_{2i}; x_{1i}^2]$ as the actual monomials of the subsystems, unknown matrices

$$A_i = \begin{bmatrix} 0 & 1 & 0 \\ 0 & 0 & 1 \end{bmatrix}, \quad B_i = \begin{bmatrix} 0 \\ 1 \end{bmatrix},$$

and the adversarial matrix partitions

$$D_{ij} = 10^{-2} \times \begin{bmatrix} 1 & 0 \\ 0 & 0 \end{bmatrix},$$

the network matrices based on Definition 2.2 are as follows

$$A = \{A_{ij}\} = \begin{cases} A_i & i = j, \\ \tilde{D}_{ij} & i = 2j \vee i = 2j + 1, \\ \mathbf{0}_{2 \times 3} & \text{Otherwise,} \end{cases}$$

$B = \text{blkdiag}(B_1, \dots, B_{2047})$.

We gather $T = 12$ samples with $\tau = 0.01$ from each subsystem (22) and select $\mathcal{F}_i(x_i) = [x_{1i}; x_{2i}; x_{1i}^2; x_{2i}^2; x_{1i} x_{2i}]$. Following the procedure outlined in Algorithm 1, we set $\kappa_i = 0.1$, $\pi_i = 0.00014535$, obtaining

$$P_i = 10^4 \times \begin{bmatrix} 4.3254 & 2.8599 \\ 2.8599 & 2.5547 \end{bmatrix},$$

$$\begin{aligned}\mathcal{V}_i(x_i) &= 43253.98 x_{1i}^2 + 57198.4261 x_{1i} x_{2i} + 25546.7906 x_{2i}^2, \\ u_i &= -x_{1i}^2 - 1.288 \times 10^{-10} x_{1i} x_{2i} - 2.5113 \times 10^{-11} x_{2i}^2 \\ &\quad - 8.4045 x_{1i} - 6.6181 x_{2i},\end{aligned}$$

with $\underline{\alpha}_i = 4.4621 \times 10^3$, $\bar{\alpha}_i = 6.4339 \times 10^4$, $\rho_i = 0.68799$, satisfying the compositional condition (19). Thus, the CLF and GAS controller for the network are designed as:

$$\mathcal{V}(x) = \sum_{i=1}^{2047} \mathcal{V}_i(x_i), \quad u = [u_1; \dots; u_{2047}],$$

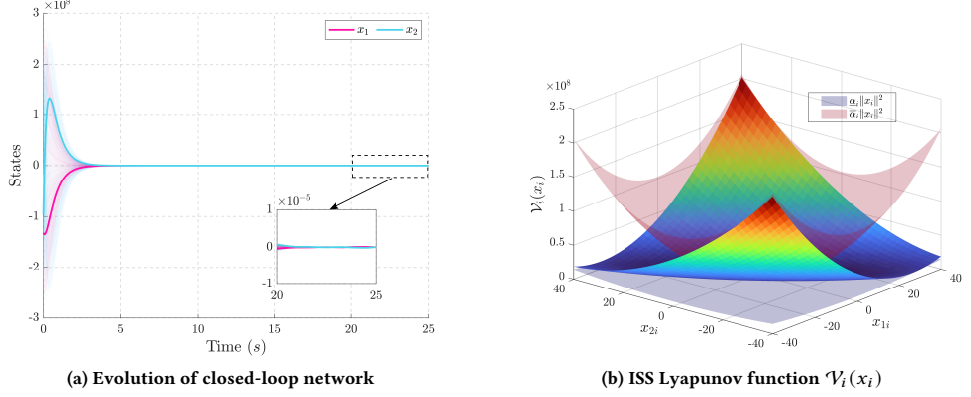


Figure 4: Interconnected academic network in a binary tree topology: (a) demonstrates the evolution of the network under the synthesized controller, highlighting the states of an arbitrary subsystem in bold and shading those of the remaining subsystems; (b) illustrates the ISS Lyapunov function $\mathcal{V}_i(x_i)$ of an arbitrary subsystem, demonstrating the fulfillment of condition (8a).

with $\underline{\alpha} = \min_i \{\underline{\alpha}_i\} = 4.4621 \times 10^3$, $\bar{\alpha} = \max_i \{\bar{\alpha}_i\} = 6.4339 \times 10^4$, $\kappa = 0.0997$. We apply the GAS controller to the network, starting from arbitrary initial conditions $x(0) \in [-2.5 \times 10^8, 2.5 \times 10^8]$, which are sufficiently large to demonstrate the effectiveness of the proposed approach. Figure 4(a) depicts the closed-loop trajectories of a representative subsystem under the synthesized controller, while Figure 4(b) visualizes the satisfaction of condition (8a).

6.4 Academic Network: Star Topology

In this subsection, we consider a network of academic dynamics, with a star topology, comprising 1000 subsystems. Each subsystem has the following dynamics

$$\begin{aligned}\dot{x}_{1i} &= x_{2i} + 10^{-2}x_{11}, \\ \dot{x}_{2i} &= x_{1i}^2 + u_i,\end{aligned}\quad (23a)$$

for $i \in \{2, \dots, 1000\}$, whereas for $i = 1$

$$\begin{aligned}\dot{x}_{11} &= x_{21}, \\ \dot{x}_{21} &= x_{11}^2 + u_1.\end{aligned}\quad (23b)$$

Hence, in compliance with Definition 2.2, the network matrices are

$$A = \{A_{ij}\} = \begin{cases} A_i & i = j, \\ \tilde{D}_{ij} & j = 1, i \neq j, \\ \mathbf{0}_{2 \times 3} & \text{Otherwise,} \end{cases} \quad B = \text{blkdiag}(B_1, \dots, B_{1000}).$$

We gather $T = 10$ samples with $\tau = 0.01$ from each subsystem (23). Following the steps in Algorithm 1, we set $\kappa_i = 1$, $\pi_i = 0.0001661$ and obtain

$$\begin{aligned}P_i &= 10^4 \times \begin{bmatrix} 4.7642 & 1.0768 \\ 1.0768 & 0.3979 \end{bmatrix}, \\ \mathcal{V}_i(x_i) &= 47641.9535x_{1i}^2 + 21535.1163x_{1i}x_{2i} + 3979.1603x_{2i}^2, \\ u_i &= -x_{1i}^2 + 5.9826 \times 10^{-11}x_{1i}x_{2i} - 2.5598 \times 10^{-11}x_{2i}^2 \\ &\quad - 41.2568x_{1i} - 11.7528x_{2i},\end{aligned}$$

with $\underline{\alpha}_i = 1.4682 \times 10^3$, $\bar{\alpha}_i = 5.0153 \times 10^4$, $\rho_i = 0.60205$, which satisfies the compositional condition (19). Hence, the CLF and GAS controller for the network are designed as

$$\mathcal{V}(x) = \sum_{i=1}^{1000} \mathcal{V}_i(x_i), \quad u = [u_1; \dots; u_{1000}],$$

with $\underline{\alpha} = \min_i \{\underline{\alpha}_i\} = 1.4682 \times 10^3$, $\bar{\alpha} = \max_i \{\bar{\alpha}_i\} = 5.0153 \times 10^4$, $\kappa = 0.5903$. We apply the GAS controller to the network, initialized with arbitrary initial conditions $x(0) \in [-2.5 \times 10^8, 2.5 \times 10^8]$, which are sufficiently large to demonstrate our proposed approach. Figure 5(a) depicts the closed-loop trajectories of a representative subsystem under the synthesized controller, while Figure 5(b) visualizes the satisfaction of condition (8a).

6.5 Lu Network: Line Topology

As for the last case study, we consider a line network of 2000 Lorenz-type systems [42], which are well-known for their chaotic solutions. Lorenz networks are used in various fields, such as climate modeling, where they help understand the dynamics of coupled atmospheric processes. They are also employed in engineering to design robust systems that can tolerate and leverage chaotic behavior, in secure communications to develop encryption schemes, and in neuroscience to model complex brain activities. The Lorenz-type systems considered here are known as Lu. Each subsystem has three states $x_i = [x_{1i}; x_{2i}; x_{3i}]$, evolving as follows

$$\begin{aligned}\dot{x}_{1i} &= -36x_{1i} + 36x_{2i} - 10^{-3}x_{1(i-1)}, \\ \dot{x}_{2i} &= 28x_{2i} - x_{1i}x_{3i} + u_i - 10^{-3}x_{2(i-1)}, \\ \dot{x}_{3i} &= -20x_{3i} + x_{1i}x_{2i} - 10^{-3}x_{3(i-1)},\end{aligned}\quad (24a)$$

for $i \in \{2, \dots, 2000\}$ while subsystem $i = 1$ evolves as

$$\begin{aligned}\dot{x}_{11} &= -36x_{11} + 36x_{21}, \\ \dot{x}_{21} &= 28x_{21} - x_{11}x_{31} + u_1, \\ \dot{x}_{31} &= -20x_{31} + x_{11}x_{21}.\end{aligned}\quad (24b)$$

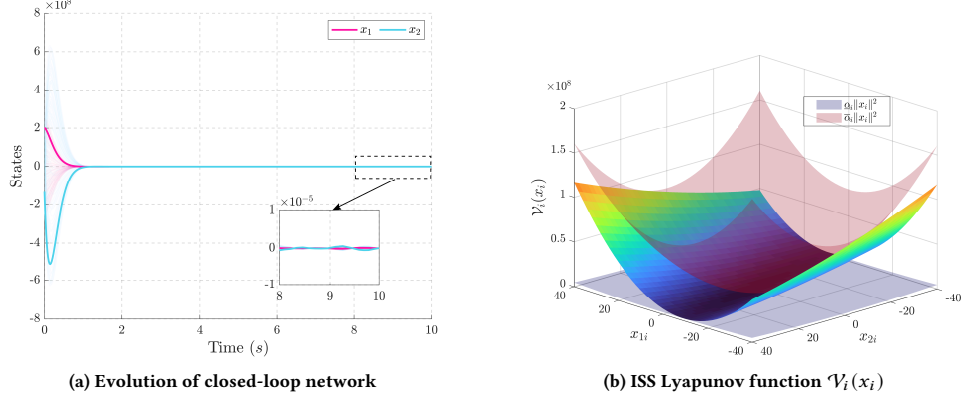


Figure 5: Interconnected academic network in a star topology: (a) demonstrates the evolution of the network under the synthesized controller, highlighting the states of an arbitrary subsystem in bold and shading those of the remaining subsystems; (b) illustrates the ISS Lyapunov function $\mathcal{V}_i(x_i)$ of an arbitrary subsystem, demonstrating the fulfillment of condition (8a).

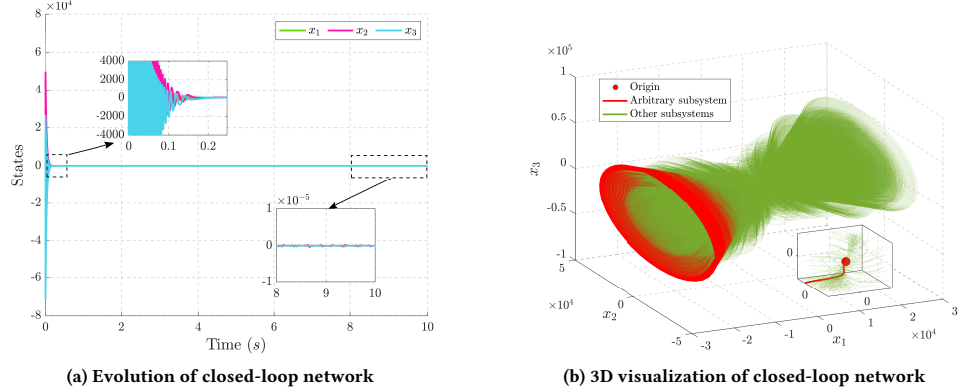


Figure 6: Interconnected Lu network in a line topology: (a) demonstrates the evolution of the network under the synthesized controller, highlighting the states of an arbitrary subsystem in bold and shading those of the remaining subsystems. (b) visualizes trajectories of the network under the synthesized controller in 3D, demonstrating that all states converge to the origin.

Therefore, with actual monomials $\mathcal{F}_i(x_i) = [x_{1i}; x_{2i}; x_{3i}; x_{1i}x_{3i}; x_{1i}x_{2i}]$, unknown system matrix and control matrix are

$$A_i = \begin{bmatrix} -36 & 36 & 0 & 0 & 0 \\ 0 & 28 & 0 & -1 & 0 \\ 0 & 0 & -20 & 0 & 1 \end{bmatrix}, \quad B_i = \begin{bmatrix} 0 \\ 1 \\ 0 \end{bmatrix},$$

and adversarial matrix partitions are

$$D_{ij} = 10^{-3} \times \begin{bmatrix} -1 & 0 & 0 \\ 0 & -1 & 0 \\ 0 & 0 & -1 \end{bmatrix}.$$

The matrices of the line network as per Definition 2.2 are as follows:

$$A = \begin{bmatrix} A_1 & \mathbf{0}_{3 \times 5} & \mathbf{0}_{3 \times 5} & \cdots & \mathbf{0}_{3 \times 5} \\ \tilde{D}_{21} & A_2 & \mathbf{0}_{3 \times 5} & \cdots & \mathbf{0}_{3 \times 5} \\ \vdots & & \ddots & & \vdots \\ \mathbf{0}_{3 \times 5} & \cdots & \tilde{D}_{1999 \ 1998} & A_{1999} & \mathbf{0}_{3 \times 5} \\ \mathbf{0}_{3 \times 5} & \cdots & \mathbf{0}_{3 \times 5} & \tilde{D}_{2000 \ 1999} & A_{2000} \end{bmatrix},$$

$$B = \text{blkdiag}(B_1, \dots, B_{2000}).$$

We collect $T = 150$ samples with a sampling time of $\tau = 10^{-4}$ from each subsystem in (24) and set $\mathcal{F}_i(x_i) = [x_{1i}; x_{2i}; x_{3i}; x_{1i}x_{3i}; x_{1i}x_{2i}; x_{2i}x_{3i}]$. Following the procedure outlined in Algorithm 1, we set

$\kappa_i = 10^{-4}$ and $\pi_i = 0.1304$, obtaining the following results:

$$P_i = \begin{bmatrix} 154.5767 & -3.0842 \times 10^{-8} & -82.5652 \\ -3.0842 \times 10^{-8} & 86.8543 & -5.0350 \times 10^{-8} \\ -82.5652 & -5.0350 \times 10^{-8} & 88.5103 \end{bmatrix},$$

$$\begin{aligned} \mathcal{V}_i(x_i) &= 154.5767x_{1i}^2 - 6.1684 \times 10^{-8}x_{1i}x_{2i} - 165.1304x_{1i}x_{3i} \\ &\quad + 86.8543x_{2i}^2 - 1.007 \times 10^{-7}x_{2i}x_{3i} + 88.5103x_{3i}^2, \\ u_i &= 0.95062x_{1i}^2 - 1.2347 \times 10^{-8}x_{1i}x_{2i} - 0.019067x_{1i}x_{3i} \\ &\quad - 1.2869 \times 10^{-7}x_{2i}^2 - 1.3213 \times 10^{-7}x_{2i}x_{3i} \\ &\quad + 2.1723 \times 10^{-9}x_{3i}^2 - 64.0693x_{1i} - 77.1287x_{2i} \\ &\quad + 34.2218x_{3i}, \end{aligned}$$

with $\underline{\alpha}_i = 32.6154$, $\bar{\alpha}_i = 210.4716$, $\rho_i = 7.671137 \times 10^{-6}$. These parameters satisfy the compositional condition (19), yielding $\underline{\alpha} = \min_i \{\underline{\alpha}_i\} = 32.6154$, $\bar{\alpha} = \max_i \{\bar{\alpha}_i\} = 210.4716$, and $\kappa = 9.9765 \times 10^{-5}$. Consequently, the CLF and GAS controller for the network are designed as

$$\mathcal{V}(x) = \sum_{i=1}^{2000} \mathcal{V}_i(x_i), \quad u = [u_1; \dots; u_{2000}].$$

We apply the GAS controller to the network with arbitrary initial conditions $x(0) \in [-25000, 25000]$. Closed-loop trajectories of a representative Lu subsystem under the synthesized controller are depicted in Figures 6(a) and 6(b).

7 Conclusion

In this work, we offered an innovative compositional data-driven methodology for synthesizing controllers that guarantee GAS over large-scale interconnected networks with unknown mathematical models. By leveraging data from subsystem trajectories and ensuring input-to-state stability through ISS Lyapunov functions, our framework effectively designed local controllers for individual subsystems. The requirement of collecting only a single input-state trajectory for each subsystem up to a specified time horizon, coupled with utilizing small-gain compositional reasoning, enabled the construction of a CLF for the entire network, thus ensuring a GAS certificate. Importantly, our approach significantly reduced the computational complexity from a polynomial to a linear scale with respect to the number of subsystems. The efficacy and practicality of our method were validated through extensive case studies on various networks with diverse interconnection topologies. Developing a compositional data-driven technique for large-scale networks to encompass a broader class of nonlinear systems beyond polynomials is being investigated as future work.

References

- [1] D. Nesić and D. Angeli, "Integral versions of ISS for sampled-data nonlinear systems via their approximate discrete-time models," *IEEE Transactions on Automatic Control*, vol. 47, no. 12, pp. 2033–2037, 2002.
- [2] A. A. Agrachev, A. S. Morse, E. D. Sontag, H. J. Sussmann, and V. I. Utkin, "Input to state stability: Basic concepts and results," *Nonlinear and optimal control theory: lectures given at the CIME summer school held in Cetraro, Italy June 19–29, 2004*, pp. 163–220, 2008.
- [3] A. Isidori, *Nonlinear control systems II*. Springer, 2013.
- [4] Z. P. Jiang, A. R. Teel, and L. Praly, "Small-gain theorem for ISS systems and applications," *Mathematics of Control, Signals and Systems*, vol. 7, pp. 95–120, 1994.
- [5] Z. P. Jiang, I. M. Mareels, and Y. Wang, "A Lyapunov formulation of the nonlinear small-gain theorem for interconnected ISS systems," *Automatica*, vol. 32, no. 8, pp. 1211–1215, 1996.
- [6] S. Dashkovskiy, B. S. Rüffer, and F. R. Wirth, "An ISS small gain theorem for general networks," *Mathematics of Control, Signals and Systems (MCSS)*, vol. 19, no. 2, pp. 93–122, 2007.
- [7] S. N. Dashkovskiy, B. S. Rüffer, and F. R. Wirth, "Small gain theorems for large scale systems and construction of ISS lyapunov functions," *SIAM Journal on Control and Optimization*, vol. 48, no. 6, pp. 4089–4118, 2010.
- [8] F. Dörfler, J. Coulson, and I. Markovsky, "Bridging direct and indirect data-driven control formulations via regularizations and relaxations," *IEEE Transactions on Automatic Control*, vol. 68, no. 2, pp. 883–897, 2022.
- [9] Z. Hou and Z. Wang, "From model-based control to data-driven control: Survey, classification and perspective," *Information Sciences*, vol. 235, pp. 3–35, 2013.
- [10] C. De Persis and P. Tesi, "Formulas for data-driven control: Stabilization, optimality, and robustness," *IEEE Transactions on Automatic Control*, vol. 65, no. 3, pp. 909–924, 2020.
- [11] M. Guo, C. De Persis, and P. Tesi, "Data-driven stabilization of nonlinear polynomial systems with noisy data," *IEEE Transactions on Automatic Control*, vol. 67, no. 8, pp. 4210–4217, 2021.
- [12] J. Berberich, J. Köhler, M. A. Müller, and F. Allgöwer, "Data-driven model predictive control with stability and robustness guarantees," *IEEE Transactions on Automatic Control*, vol. 66, no. 4, pp. 1702–1717, 2020.
- [13] A. J. Taylor, V. D. Dorobantu, S. Dean, B. Recht, Y. Yue, and A. D. Ames, "Towards robust data-driven control synthesis for nonlinear systems with actuation uncertainty," in *Proceedings of the 60th Conference on Decision and Control (CDC)*. IEEE, 2021, pp. 6469–6476.
- [14] J. Harrison, A. Sharma, R. Calandra, and M. Pavone, "Control adaptation via meta-learning dynamics," in *Workshop on Meta-Learning at NeurIPS*, vol. 2018, 2018.
- [15] D. Žikelić, M. Lechner, A. Verma, K. Chatterjee, and T. Henzinger, "Compositional policy learning in stochastic control systems with formal guarantees," *Advances in Neural Information Processing Systems*, vol. 36, 2024.
- [16] J. Kenanian, A. Balkan, R. M. Jungers, and P. Tabuada, "Data driven stability analysis of black-box switched linear systems," *Automatica*, vol. 109, 2019.
- [17] N. Boffi, S. Tu, N. Matni, J. J. Slotine, and V. Sindhwani, "Learning stability certificates from data," in *Proceedings of Conference on Robot Learning*. PMLR, 2021, pp. 1341–1350.
- [18] A. Lavaei, P. M. Esfahani, and M. Zamani, "Data-driven stability verification of homogeneous nonlinear systems with unknown dynamics," in *IEEE 61st Conference on Decision and Control (CDC)*, 2022, pp. 7296–7301.
- [19] R. Zhou, T. Quartz, H. De Sterck, and J. Liu, "Neural lyapunov control of unknown nonlinear systems with stability guarantees," *Advances in Neural Information Processing Systems*, vol. 35, pp. 29 113–29 125, 2022.
- [20] H. Chen, A. Bisoffi, and C. De Persis, "Data-driven input-to-state stabilization," *arXiv preprint arXiv:2407.06044*, 2024.
- [21] M. Zaker, D. Angeli, and A. Lavaei, "Certified learning of incremental iss controllers for unknown nonlinear polynomial dynamics," *arXiv: 2412.03901*, 2024.
- [22] M. Sperl, J. Mysliwitz, and L. Grüne, "Approximation of separable control lyapunov functions with neural networks," 2023.
- [23] J. Liu, Y. Meng, M. Fitzsimmons, and R. Zhou, "Compositionally verifiable vector neural lyapunov functions for stability analysis of interconnected nonlinear systems," *arXiv preprint arXiv:2403.10007*, 2024.
- [24] S. Zhang, Y. Xiu, G. Qu, and C. Fan, "Compositional neural certificates for networked dynamical systems," in *Learning for Dynamics and Control Conference*. PMLR, 2023, pp. 272–285.
- [25] A. Lavaei and D. Angeli, "Data-driven stability certificate of interconnected homogeneous networks via ISS properties," *IEEE Control Systems Letters*, vol. 7, pp. 2395–2400, 2023.
- [26] L. De Moura and N. Bjørner, "Z3: An efficient SMT solver," in *Proceedings of the International conference on Tools and Algorithms for the Construction and Analysis of Systems*, 2008, pp. 337–340.
- [27] S. Gao, J. Avigad, and E. M. Clarke, "δ-complete decision procedures for satisfiability over the reals," in *Automated Reasoning*, ser. Lecture Notes in Computer Science, 2012, pp. 286–300.
- [28] A. Cimatti, A. Griggio, and R. Schaafsma, B. J. and Sebastiani, "The MathSAT5 SMT solver," in *Tools and Algorithms for the Construction and Analysis of Systems*, ser. Lecture Notes in Computer Science, 2013, pp. 93–107.
- [29] T. Wongpiromsarn, U. Topcu, and A. Lamperski, "Automata theory meets barrier certificates: Temporal logic verification of nonlinear systems," *IEEE Transactions on Automatic Control*, vol. 61, no. 11, pp. 3344–3355, 2015.
- [30] A. Abate, A. Edwards, and M. Giacobbe, "Neural abstractions," *Advances in Neural Information Processing Systems*, vol. 35, pp. 26 432–26 447, 2022.
- [31] G. C. Calafiore and M. C. Campi, "The scenario approach to robust control design," *IEEE Transactions on Automatic Control*, vol. 51, no. 5, pp. 742–753, 2006.
- [32] D. Angeli, E. D. Sontag, and Y. Wang, "A characterization of integral input-to-state stability," *IEEE Transactions on Automatic Control*, vol. 45, no. 6, pp. 1082–1097, 2000.

- [33] E. D. Sontag and Y. Wang, "New characterizations of input-to-state stability," *IEEE transactions on automatic control*, vol. 41, no. 9, pp. 1283–1294, 1996.
- [34] E. K. Larsson, M. Mossberg, and T. Söderström, "Estimation of continuous-time stochastic system parameters," in *Identification of continuous-time models from sampled data*. Springer, 2008, pp. 31–66.
- [35] A. Padoan and A. Astolfi, "Towards deterministic subspace identification for autonomous nonlinear systems," in *Proceedings of the 54th Conference on Decision and Control (CDC)*. IEEE, 2015, pp. 127–132.
- [36] J. C. Willems, P. Rapisarda, I. Markovsky, and B. L. De Moor, "A note on persistency of excitation," *Systems & Control Letters*, vol. 54, no. 4, pp. 325–329, 2005.
- [37] R. Bhatia and C. Davis, "A cauchy-schwarz inequality for operators with applications," *Linear algebra and its applications*, vol. 223, pp. 119–129, 1995.
- [38] W. H. Young, "On classes of summable functions and their Fourier series," *Proceedings of the Royal Society of London A: Mathematical, Physical and Engineering Sciences*, vol. 87, no. 594, pp. 225–229, 1912.
- [39] A. Papachristodoulou, J. Anderson, G. Valmorbida, S. Prajna, P. Seiler, and P. Parrilo, "SOSTOOLS version 3.00 sum of squares optimization toolbox for MATLAB," *arXiv:1310.4716*, 2013.
- [40] J. F. Sturm, "Using sedumi 1.02, a matlab toolbox for optimization over symmetric cones," *Optimization methods and software*, vol. 11, no. 1-4, pp. 625–653, 1999.
- [41] H. K. Khalil, *Control of nonlinear systems*. 2002.
- [42] S. H. Strogatz, *Nonlinear dynamics and chaos: With applications to physics, biology, chemistry, and engineering*. CRC press, 2018.